CHEMISTRY OF MATERIALS
Article

Chem. Mater. **2010,** *22,* 6453–6458 6453
DOI:10.1021/cm1027095

The Longest β-Unsubstituted Oligothiophenes and Their Self-Assembly in Solution

Andreas Kreyes,[†] Masoud Amirkhani,[‡] Ingo Lieberwirth,[§] Ralf Mauer,[§] Frederic Laquai,[§] Katharina Landfester,[†,§] and Ulrich Ziener*[,†]

[†]*Institute of Organic Chemistry III, University of Ulm, Albert-Einstein-Allee 11, D-89081 Ulm, Germany,* [‡]*Institute of Experimental Physics, University of Ulm, Albert-Einstein-Allee 11, D-89081 Ulm, Germany, and* [§]*Max Planck Institute for Polymer Research, Ackermannweg 10, 55128 Mainz, Germany*

Received September 20, 2010. Revised Manuscript Received October 15, 2010

β-Unsubstituted oligothiophenes with up to 13 thiophene units are described. These represent the longest oligomers ever reported in this class. In solution, those compounds show a temperature- and concentration-dependent aggregation behavior. Absorption, fluorescence, dynamic light scattering, and cryo-transmission electron microscopy investigations reveal the formation of wormlike aggregates several hundred nanometers in length and ca. 5 nm in width.

Introduction

For more than 25 years, the development of novel organic semiconductors for use in electronic devices has been a focus of scientific research. Applications of such materials containing conjugated π-electron systems include solar cells, organic field-effect transistors (OFETs), organic light-emitting diodes (OLEDs),[1] organic light-emitting transistors (OLETs),[2] radio frequency identification (RFID) tags,[3] and sensors for gases and biomolecules.[4] A major advantage of organic semiconductors over silicon is the possibility to engineer the properties, such as band gap, molecular ordering, and processability.[1a,5] One of the most promising classes of materials are α,ω-substituted oligothiophenes. Ideal candidates are long oligomers with solubilizing end groups for processability. In the literature, mainly systems up to seven thiophene units are reported,[6] and there are only a few examples exceeding this number.[7] In contrast, β-substituted oligomers are known up to a 96-mer.[8] The longest oligothiophenes without β-substituents ever described bear 11 units.[7a,b] Synthetic drawbacks are responsible for the few examples with more than seven thiophene rings. Besides the length of the oligomers, their ordering in solid state is a prerequisite for high performance in thin-film devices.[5c,9] There are attractive processing techniques for thin films, such as printing, which require (i) sufficient solubility and (ii) ideally preordering of the

*Author to whom correspondence should be addressed. E-mail: ulrich.ziener@uni-ulm.de.

(1) (a) Roncali, J.; Leriche, P.; Cravino, A. *Adv. Mater.* **2007**, *19*, 2045–2060. (b) Barbarella, G.; Melucci, M.; Sotgiu, G. *Adv. Mater.* **2005**, *17*, 1581–1593. (c) Lloyd, M. T.; Anthony, J. E.; Malliaras, G. G. *Mater. Today* **2007**, *10*, 34–41. (d) Allard, S.; Forster, M.; Souharce, B.; Thiem, H.; Scherf, U. *Angew. Chem., Int. Ed.* **2008**, *47*, 4070–4098. (e) Reese, C.; Roberts, M.; Ling, M. M.; Bao, Z. *Mater. Today* **2004**, *7*, 20–27.
(2) Cicoira, F.; Santato, C.; Melucci, M.; Favaretto, L.; Gazzano, M.; Muccini, M.; Barbarella, G. *Adv. Mater.* **2006**, *18*, 169–174.
(3) (a) Baude, P. F.; Ender, D. A.; Haase, M. A.; Kelley, T. W.; Muyres, D. V.; Theiss, S. D. *Appl. Phys. Lett.* **2003**, *82*, 3964–3966. (b) Voss, D. *Nature* **2000**, *407*, 442–444.
(4) (a) Torsi, L.; Cioffi, N.; Di Franco, C.; Sabbatini, L.; Zambonin, P. G.; Bleve-Zacheo, T. *Solid-State Electron.* **2001**, *45*, 1479–1485. (b) Zhu, Z. T.; Mason, J. T.; Dieckmann, R.; Malliaras, G. G. *Appl. Phys. Lett.* **2002**, *81*, 4643–4645. (c) Sokolov, A. N.; Roberts, M. E.; Bao, Z. *Mater. Today* **2009**, *12*, 12–20.
(5) (a) Beaujuge, P. M.; Ellinger, S.; Reynolds, J. R. *Nat. Mater.* **2008**, *7*, 795–799. (b) Oliva, M. M.; Casado, J.; Raposo, M. M. M.; Fonseca, A. M. C.; Hartmann, H.; Hernandez, V.; Lopez Navarrete, J. T. *J. Org. Chem.* **2006**, *71*, 7509–7520. (c) Halik, M.; Klauk, H.; Zschieschang, U.; Schmid, G.; Ponomarenko, S.; Kirchmeyer, S.; Weber, W. *Adv. Mater.* **2003**, *15*, 917–922.
(6) (a) Henze, O.; Feast, W. J.; Gardebien, F.; Jonkheijm, P.; Lazzaroni, R.; Leclère, P.; Meijer, E. W.; Scheming, A. P. H. J. *J. Am. Chem. Soc.* **2006**, *128*, 5923–5929. (b) Murphy, A. R.; Fréchet, J. M. J.; Chang, P.; Lee, J.; Subramanian, V. *J. Am. Chem. Soc.* **2004**, *126*, 1596–1597. (c) Afzali, A.; Breen, T. L.; Kagan, C. R. *Chem. Mater.* **2002**, *14*, 1742–1746. (d) Yasuda, T.; Ooi, H.; Morita, J.; Akama, Y.; Minoura, K.; Funahashi, M.; Shimomura, T.; Kato, T. *Adv. Funct. Mater.* **2009**, *19*, 411–419. (e) Videlot-Ackermann, C.; Ackermann, J.; Brisset, H.; Kawamura, K.; Yoshimoto, N.; Raynal, P.; Kassmi, A. E.; Fages, F. *J. Am. Chem. Soc.* **2005**, *127*, 16346–16347. (f) Sakamoto, K.; Takashima, Y.; Yamaguchi, H.; Harada, A. *J. Org. Chem.* **2007**, *72*, 459–465. (g) Facchetti, A.; Yoon, M. H.; Stern, C. L.; Hutchison, G. R.; Ratner, M. A.; Marks, T. J. *J. Am. Chem. Soc.* **2004**, *126*, 13480–13501. (h) Kreyes, A.; Ellinger, S.; Landfester, K.; Defaux, M.; Ivanov, D. A.; Elschner, A.; Meyer-Friedrichsen, T.; Ziener, U. *Chem. Mater.* **2010**, *22*, 2079–2092.
(7) (a) Hempenius, M. A.; Langeveld-Voss, B. M. W.; Van Haare, J. A. E. H.; Janssen, R. A. J.; Sheiko, S. S.; Spatz, J. P.; Möller, M.; Meijer, E. W. *J. Am. Chem. Soc.* **1998**, *120*, 2798–2804. (b) Ellinger, S.; Kreyes, A.; Ziener, U.; Hoffmann-Richter, C.; Landfester, K.; Möller, M. *Eur. J. Org. Chem.* **2007**, 5686–5702. (c) Hajlaoui, R.; Fichou, D.; Horowitz, G.; Nessakh, B.; Constant, M.; Garnier, F. *Adv. Mater.* **1997**, *9*, 557–561. (d) DeLongchamp, D. M.; Jung, Y.; Fischer, D. A.; Lin, E. K.; Chang, P.; Subramanian, V.; Murphy, A. R.; Fréchet, J. M. J. *J. Phys. Chem. B* **2006**, *110*, 10645–10650.
(8) Izumi, T.; Kobashi, S.; Takimiya, K.; Aso, Y.; Otsubo, T. *J. Am. Chem. Soc.* **2003**, *125*, 5286–5287.
(9) (a) Janssen, P. G. A.; Pouderoijen, M.; Van Breemen, A. J. J. M.; Herwig, P. T.; Koeckelberghs, G.; Popa-Merticaru, A. R.; Meskers, S. C. J.; Valeton, J. J. P.; Meijer, E. W.; Schenning, A. P. H. J. *J. Mater. Chem.* **2006**, *16*, 4335–4342. (b) Vaidyanathan, S.; Dötz, F.; Katz, H. E.; Lawrentz, U.; Granstrom, J.; Reichmanis, E. *Chem. Mater.* **2007**, *19*, 4676–4681.

Published on Web 11/08/2010

Scheme 1. Synthesis of the Branched Silane Substituent

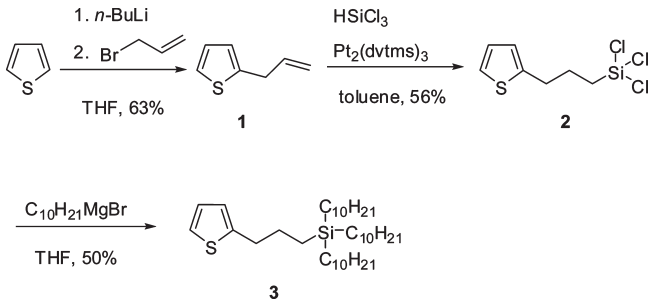

molecules already in solution. Thus, it is desirable to target self-assembling oligomers with long thiophene cores, which still show reasonable solubilities.

Here, we report on the synthesis of the longest oligothiophenes ever described, with 11 and 13 thiophene units, respectively equipped with solubilizing branched alkyl chains in the α- and ω-positions. Their self-assembly behavior in an organic solvent is characterized by time-resolved optical spectroscopy, dynamic light scattering (DLS), and cryo-transmission electron microscopy (cryo-TEM), which reveal the formation of wormlike aggregates in the size range of hundreds of nanometers.

Results and Discussion

Synthesis (see the Supporting Information). The synthetic route toward undecathiophene (**16**) and tridecathiophene (**17**) starts with the construction of the carbosilane substituent attached to the thiophene core (see Scheme 1). First, thiophene was lithiated with *n*-BuLi and then monoalkenylated with allylbromide. The olefinic double bond of resulting 2-allylthiophene (**1**) was hydrosilylated subsequently with trichlorosilane under platinum catalysis. The resulting intermediate product (**2**) was converted to the desired monosubstituted thiophene (**3**) by a 3-fold alkylation with decylmagnesiumbromide. In the second part of the synthesis, monosubstituted oligomers were built by a series of Stille-type couplings (see Scheme 2). After lithiation and stannylation, substituted thiophene **3** was coupled with 2-bromothiophene and 5-bromoterthiophene, respectively, to give the corresponding bithiophene **5** and quaterthiophene **6**, respectively. Quinquethiophene **8** was obtained by repeated stannylation of **5** and consecutive coupling with 5-bromoterthiophene. Subsequently, the monosubstituted oligomers **6** and **8** were again stannylated and converted to soluble undecathiophene and tridecathiophene precursors (**12** and **13**, respectively) by Stille-type coupling with brominated diketal **11** (see Scheme 3). Because of the interrupted π-conjugation and the remarkable solubilizing capacity of the bulky substituent, these compounds are still very soluble in organic solvents, so that they could be readily transformed to the corresponding 1,4-diketones (**14** and **15**) via treatment with hydrochloric acid. The solubility of the latter compounds is significantly reduced compared to the diketal precursors (especially in the case of diketone **15**); nevertheless, both could be converted to undecathiophene **16** and tridecathiophene **17**, using Lawesson's reagent as a well-established ring

Scheme 2. Stille-Type Coupling Reactions to Monosubstituted Oligomers

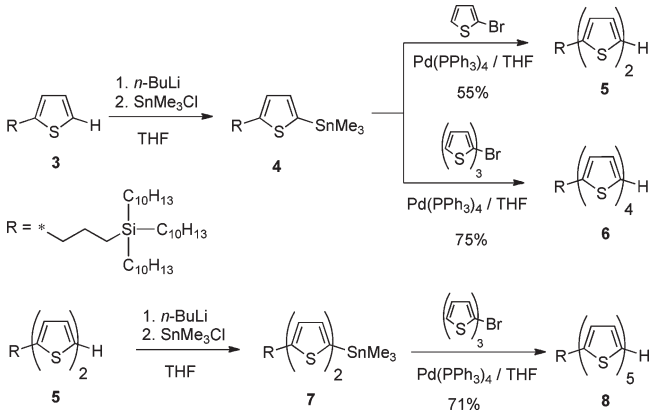

closure agent for 1,4-diketones.[10] For the synthesis of the latter, the solvent had to be changed from tetrahydrofuran (THF) to 1,1,2,2-tetrachloroethane (TCE).

Ultraviolet/Visible Light (UV/vis) Absorption and Fluorescence Spectroscopy. Temperature- and concentration-dependent UV/vis absorption and fluorescence spectroscopy were conducted with freshly prepared solutions of compounds **16** and **17** in TCE, because it proved to be the best solvent for such long oligomers. Absorption spectra of undecathiophene **16** are depicted in Figure 1a. At high temperatures, a broad and unstructured band with a maximum λ_{max} at 475 nm is observed, which is common for flexible molecules such as oligothiophenes. Cooling results in a distinct change of the spectral shape. A vibronic fine structure at the low-energy side of the spectrum with the 0−0 transition at 570 nm now becomes visible. This change is caused by the formation of aggregates in solution. Here, the molecules are forced into a stiff and planar conformation. The intramolecular overlap of π-orbitals is optimized and, therefore, the spectrum is shifted to higher wavelengths. Similarly, tridecathiophene **17** also exhibits a broad and unstructured spectrum at high temperatures, with λ_{max} being observed at almost the same wavelength (476 nm) as the shorter homologue **16** (see Figure 1b). This means that, despite two additional monomer units in **17**, the effective conjugation length in the molecular dissolved state is almost the same. Upon cooling, **17** also forms aggregates. This process already starts at much higher temperature, compared to that for **16**, because of stronger intermolecular π-interactions in the longer homologue. As can be seen in Figure 1b, the vibronic fine structure is, by far, more pronounced for **17** than for **16**. In addition, the bathochromic shift of the spectrum turns out to be larger in **17**. The 0−0 absorption band emerges at 585 nm and, thus, is red-shifted by 450 cm^{-1}, compared to that for **16**, and therefore already is very close to that of β-substituted

(10) (a) Wynberg, H.; Metselaar, J. *Synth. Commun.* **1984**, *14*, 1–9. (b) Wynberg, H.; Wiersum, U. E. *J. Org. Chem.* **1965**, *30*, 1058–1060. (c) Scheeren, J. W.; Ooms, P. H. J.; Nivard, R. J. F. *Synthesis* **1973**, 149. (d) Shridhar, D. R.; Jogibhukta, M.; Rao, P. S.; Handa, V. K. *Synthesis* **1982**, 1061–1062.

Scheme 3. Stille-Type Coupling to the Soluble Diketal Precursors, Deprotection of the Diketones, and Ring Closure to the Undecathiophene (16) and Tridecathiophene (17)

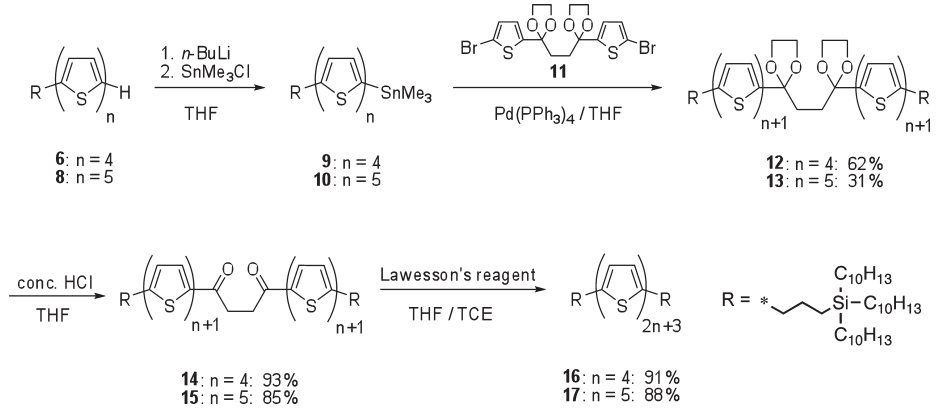

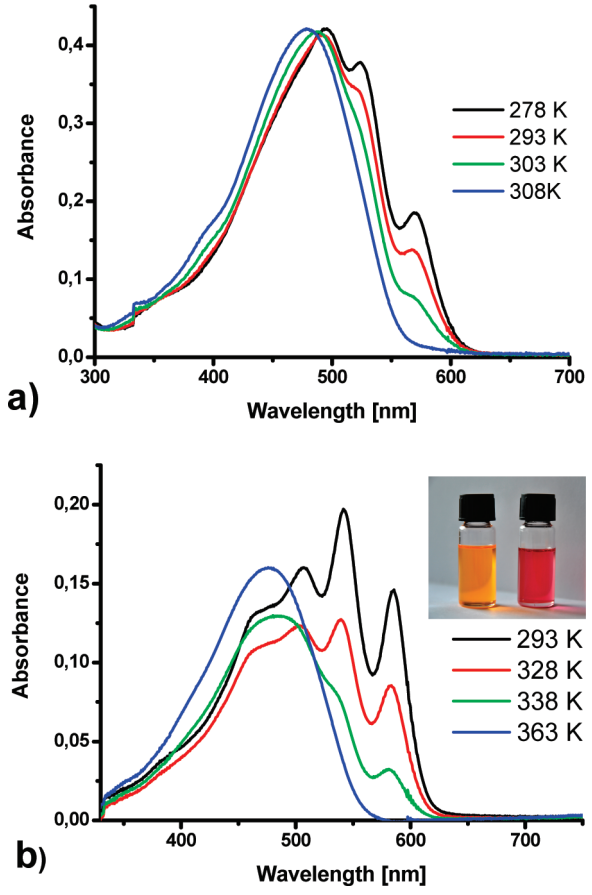

Figure 1. Absorption spectra of (a) **16** and (b) **17**; inset shows the thermochromism of **17** (left, hot solution; right, cold solution).

polythiophenes.[11] This clearly shows that the effective conjugation length in aggregates is continuously increased in the homologues series at least up to the 13-mer. This is not the case for single molecules, where torsion around the inter-ring single bonds can take place. Because of the large temperature-dependent differences in the spectral shape of **17**, the reversible transition between the molecularly dissolved state and the aggregated state can easily be observed by eye (Figure 1b, inset).

Further investigations on the temperature dependence of the equilibrium between single molecules and aggregates in solution were performed by steady-state and time-resolved fluorescence spectroscopy. Figures 2a and 2b show the steady-state emission spectra of **16** and **17**, respectively, whereas Figure 2c shows the time-integrated and normalized photoluminescence of **17**, obtained from a streak camera experiment.

Both oligomers exhibit very similar photoluminescence spectra. At high temperatures, when the molecules are molecularly dissolved and aggregation is suppressed, a distinct vibronic fine structure (0−0 absorption band, 560 nm; 0−1 absorption band, 605 nm; 0−2 absorption band, 660 nm), in conjunction with a high fluorescence intensity, was observed. In contrast to the absorption spectra, no additional bands appear upon cooling but significant quenching of the fluorescence takes place (see Figure 2). In addition, a change in the relative intensities of the three vibronic progressions was found. A closer look at this behavior was performed using time-resolved fluorescence spectroscopy (see Figure 3).

A monoexponential decay (with relaxation times of 620 ps (**16**) and 580 ps (**17**)) was found in the entire temperature range when probing the 0−0 transition, i.e., at a spectral position where mainly the fluorescence of molecularly dissolved molecules is present. At the 0−1 and 0−2 vibronic progressions, this behavior was only observed at high temperatures. At low temperatures, the relaxation turns into a biexponential decay, and a second, faster component, with a lifetime in the order of 100 ps, was observed. This transition occurs already at higher temperatures in the case of **17**, compared to **16**, and is also more pronounced for **17**, as can be estimated from the relative amplitude of the long- and short-lived components. This suggests that, for **17** (**16**), at a temperature of 278 K, 60% (40%) of the emission originates from aggregates. Furthermore, the second component is responsible for the relative increase of the 0−1 and 0−2 bands in the spectra, and we assume that this component arises from weakly fluorescent aggregates. At low temperatures, the fluorescence spectrum is a superposition

(11) (a) Zen, A.; Saphiannikova, M.; Neher, D.; Asawapirom, U.; Scherf, U. *Chem. Mater.* **2005**, *17*, 781–786. (b) Roux, C.; Leclerc, M. *Chem. Mater.* **1994**, *6*, 620–624. (c) Faid, K.; Frechette, M.; Ranger, M.; Mazerolle, L.; Levesque, I.; Leclerc, M.; Chen, T. A.; Rieke, R. D. *Chem. Mater.* **1995**, *7*, 1390–1396.

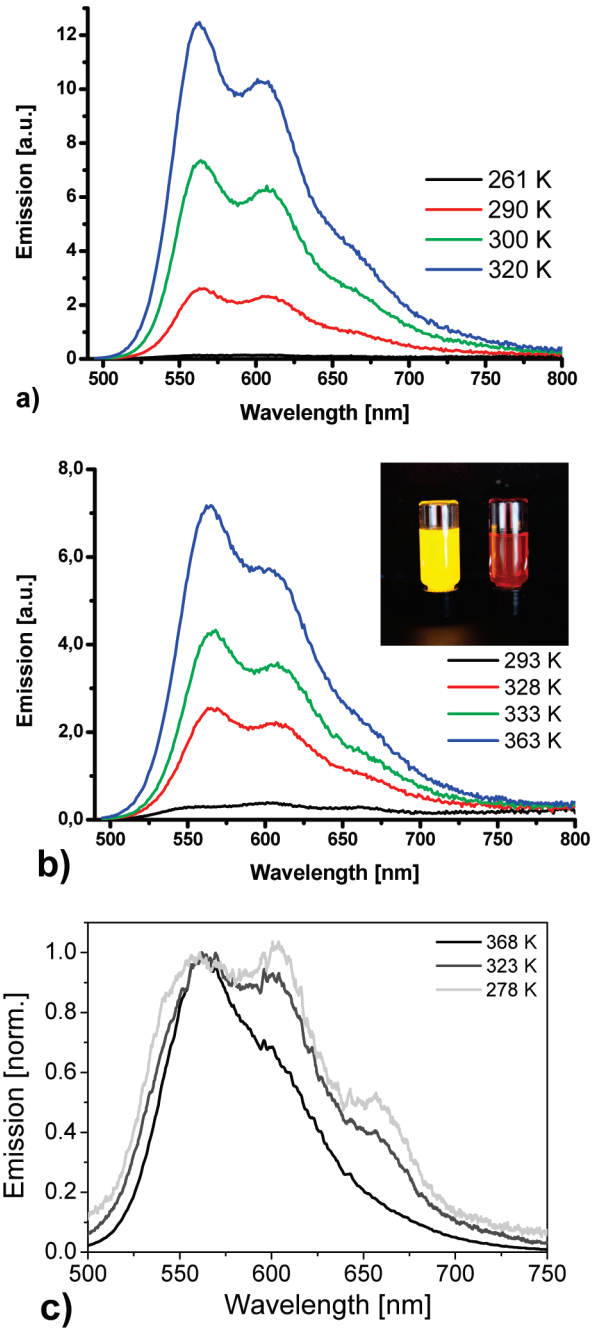

Figure 2. Steady-state fluorescence spectra of (a) **16** and (b) **17**, inset: thermochromism of **17** under a laboratory UV lamp (366 nm) (left, hot solution; right, cold solution). (c) Normalized time-integrated fluorescence spectra of **17** at different temperatures.

of the fluorescence from residual free molecules with clear 0−0, 0−1, and 0−2 vibronic progressions and a broad, red-shifted and rather unstructured fluorescence from aggregates. Even though a substantial part of the emission of the free molecules at 560 nm overlaps with the absorption of aggregates at 570 nm for **16** and 585 nm for **17**, no indications of self-absorption, which otherwise would have strongly suppressed a significant part of the spectrum, could be observed during the measurements. The most likely reason for this is the low concentration of the material in solution.

The quenching of fluorescence mentioned above follows a sigmoidal progression (Figure 4), which was also

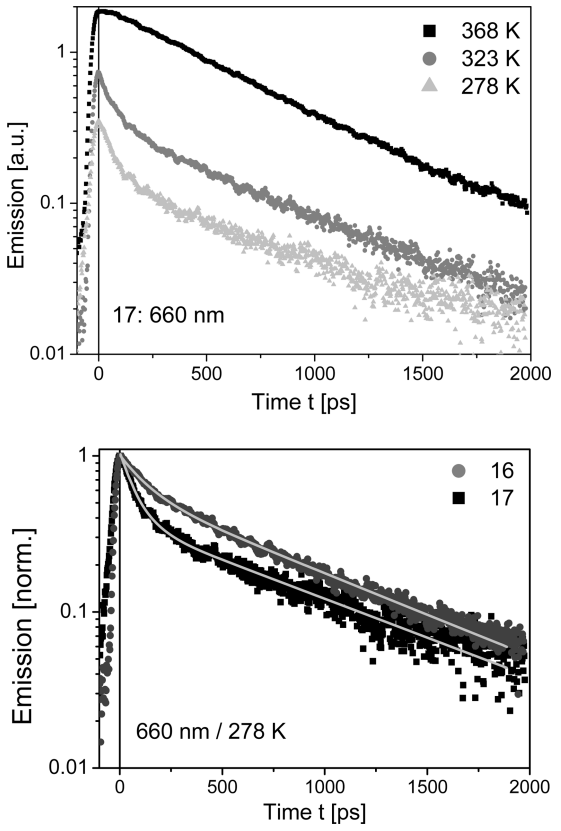

Figure 3. (Top) Fluorescence decay for **17** at various temperatures; (bottom) comparison of the fluorescence decay between **16** and **17**. (Conditions: 660 nm, 278 K, and a concentration of 5×10^{-6} mol L^{-1}.)

observed previously for the aggregation of other π-conjugated systems.[12]

The inflection points of these S-curves represent the dissociation temperature (T_{dis}) of the aggregates. T_{dis} increases as the concentration increases, which shows that the dissociation of the aggregates is an endothermic process. From such S-curves, the aggregation number (n) and/or aggregation enthalpy ΔH_{aggr} and entropy ΔS_{aggr} have been calculated in the literature. These approaches are based on models developed to describe the self-assembling properties of molecules (for example, the dimerization of DNA strands).[13] In these models (e.g., the "Equal K Model" (from ref 14)), n, ΔH_{aggr}, and ΔS_{aggr} are assumed to be independent from temperature and concentration, which means that an equilibrium between single molecules and aggregates of well-defined sizes is present. To determine if these simplifications are acceptable, we performed temperature- and concentration-dependent dynamic light scattering (DLS) on the aggregates in solution (see Figure 5).

(12) (a) Würthner, F.; Chen, Z.; Hoeben, F. J. M.; Osswald, P.; You, C. C.; Jonkheijm, P.; Herrikhuyzen, J. V.; Schenning, A. P. H. J.; Van Der Schoot, P. P. A. M.; Meijer, E. W.; Beckers, E. H. A.; Meskers, S. C. J.; Janssen, R. A. J. *J. Am. Chem. Soc.* **2004**, *126*, 10611–10618. (b) Jonkheijm, P.; Hoeben, F. J. M.; Kleppinger, R.; Van Herrikhuyzen, J.; Schenning, A. P. H. J.; Meijer, E. W. *J. Am. Chem. Soc.* **2003**, *125*, 15941–15949. (c) Apperloo, J. J.; Janssen, R. A. J.; Malenfant, P. R. L.; Frechet, J. M. J. *Macromolecules* **2000**, *33*, 7038–7043.
(13) Marky, L. A.; Breslauer, K. J. *Biopolymers* **1987**, *26*, 1601−1620.
(14) Martin, R. B. *Chem. Rev.* **1996**, *96*, 3043–3064.

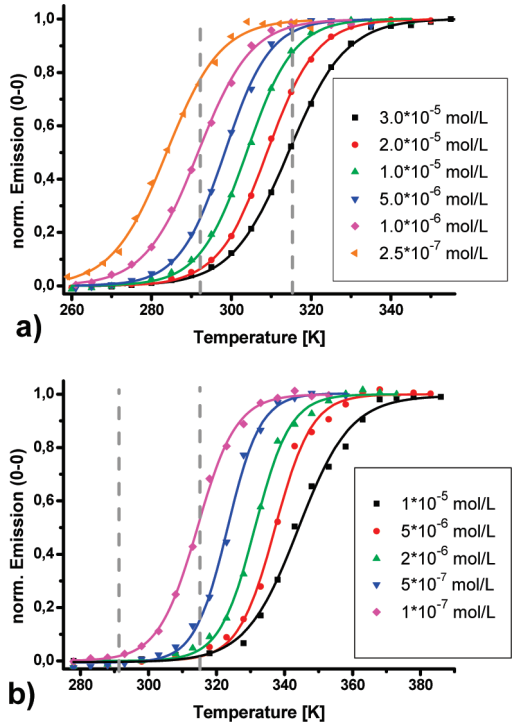

Figure 4. S-curves of (a) **16** and (b) **17**; the dashed gray lines represent the accessible temperature range for dynamic light scattering (DLS).

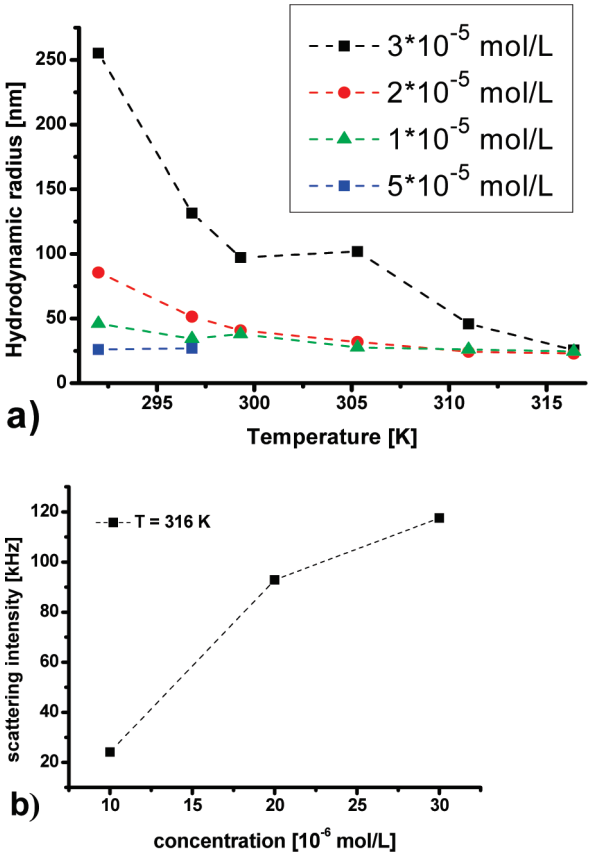

Figure 5. (a) Hydrodynamic radii of aggregates of **16** in TCE obtained from DLS measurements; (b) scattering intensity at 316 K.

The accessible temperature range was 290−316 K. In contrast to **17** the fluorescence intensity of solutions of **16** change considerably within this window (see Figure 4). Hence, we decided to conduct measurements only with the 11-mer **16** at four different concentrations (between 5×10^{-6} mol L^{-1} and 3×10^{-5} mol L^{-1}), whereas the lowest concentration yielded sufficient scattering intensity only at the two lowest temperatures. At 316 K, the other three solutions gave similar hydrodynamic radii (R_h) of 23−26 nm. The resulting scattering intensities qualitatively show that, at higher concentration, more aggregates are present. Reducing the temperature leads to larger aggregates, but the increase in R_h is strongly dependent on the concentration. Upon cooling to 292 K, R_h is doubled to 46 nm for the solution of 1×10^{-5} mol L^{-1}, whereas it is increased approximately 10-fold to 255 nm at 3×10^{-5} mol L^{-1}. These findings clearly show that, at least for the presented systems in this report, the assumptions made to calculate thermodynamic parameters of the aggregation do not mirror the real circumstances of the self-assembly of oligothiophenes properly.

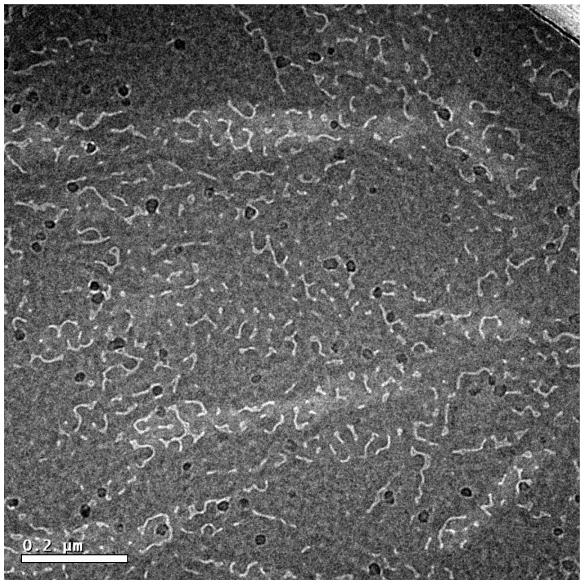

Figure 6. Cryo transmission electron microscopy (cryo-TEM) micrograph of **17** in TCE. Because of the organic solvent, the aggregates appear bright against the dark background of the vitrified TCE.

A powerful tool to visualize aggregates is electron microscopy. Figure 6 shows a cryo transmission electron microscopy (cryo-TEM) micrograph of a solution ($c = 2 \times 10^{-5}$ mol L^{-1}) of **17** in TCE shock-frozen from room temperature. Under those conditions, the molecules are expected to be in the aggregated state, according to optical spectroscopy (see Figure 4b). As is typical for cryo-TEM images of organic solutions, the contrast is inverted and, hence, the sample appears bright against the darker background of the TCE. The aggregates exhibit a wormlike shape, with a length of several hundred nanometers. The width of these "worms" is ~5 nm, which is in the range of the length of a single molecule in stretched conformation. Hence, we assume that "single-stranded" aggregates are present in solution.

Conclusion

The longest β-unsubstituted oligothiophenes ever reported, with up to 13 thiophene units, have been presented.

A ring closure/coupling chemistry approach allowed the preparation of an undecathiophene and a tridecathiophene with high purity and yield on the scale of several hundred milligrams. Branched alkyl end groups ensure sufficient solubility in common organic solvents. Intermolecular interactions of the heteroaromatic units cause the molecules to strongly aggregate in solution. Temperature- and concentration-dependent measurements reveal an S-shaped aggregation behavior. The aggregates are characterized by absorption, steady-state and transient fluorescence spectroscopy, dynamic light scattering (DLS), and cryo transmission electron microscopy (cryo-TEM), which reveal the presence of wormlike nano-objects several hundred nanometers in length and ca. 5 nm in width. In contrast to literature reports on similar but shorter oligomers, our oligothiophenes formed more and larger aggregates at a lower temperature. The present results prove that the synthetic concept, which already has been shown previously for oligothiophenes up to 11 units, can be successfully applied to longer oligomers, and we believe that, with a suitable choice of substituents, it can be extended even further. Such long oligomers shall act as suitable model compounds for unsubstituted polythiophene, with respect to electronic properties and aggregation behavior. The aggregation mechanism shall further help to understand and improve the process of film formation from solution for electronic applications such as organic field-effect transistors (OFETs).

Experimental Section

Experimental details are given in the Supporting Information.

Acknowledgment. Prof. Othmar Marti is acknowledged for fruitful discussions. We gratefully acknowledge support of the present work by the Deutsche Forschungsgemeinschaft (DFG, ZI 567/4-1). F.L. thanks the Max Planck Society for funding a Max Planck Research Group and R.M. thanks the Max Planck Graduate Center for a scholarship.

Supporting Information Available: Steady-state UV/vis and fluorescence spectroscopy, transient fluorescence spectroscopy, dynamic light scattering, cryo-transmission electron microscopy, and experimental details for the synthesis of all new compounds. This information is available free of charge via the Internet at http://pubs.acs.org.